

# Unconventional Superconductivity in $\text{UPd}_2\text{Al}_3$ from Realistic Selfconsistent Calculations

P. M. Oppeneer<sup>1</sup> and G. Varelogiannis<sup>2,3</sup>

<sup>1</sup>*Institute of Solid State and Materials Research, P.O. Box 270016, D-01171 Dresden, Germany*

<sup>2</sup>*Institute of Electronic Structure and Laser, FORTH, P.O. Box 1527, 71110 Heraklion, Greece*

<sup>3</sup>*Max-Planck-Institute for the Physics of Complex Systems, Nöthnitzer Str. 38, D-01187 Dresden, Germany*  
(November 20, 2018)

Realistic selfconsistent calculations of unconventional superconductivity in a heavy-fermion material are reported. Our calculations for  $\text{UPd}_2\text{Al}_3$  start from accurate energy band dispersions that are computed within the local spin-density functional theory and provide Fermi surfaces in agreement with experiment. Using physically motivated, realistic pairing potentials it is shown that the superconducting gap has two lines of nodes around the  $z$ -axis, thus exhibiting  $d$ -wave symmetry in the  $A_{1g}$  representation of the  $D_{6h}$  point group. Our results suggest that in a superconductor with gap nodes, the prevailing gap symmetry is dictated by the constraint that *nodes must be as far as possible from high-density areas*.

PACS numbers: 74.25.Jb, 74.20.-z

Superconductivity (SC) in heavy-fermion (HF) materials exhibits a fascinating complexity of phenomena [1]. The nature of the SC state is mostly anticipated to be unconventional, i.e., an additional symmetry is broken in the SC state, and the order parameter is therefore not the conventional spin singlet  $s$ -wave type [2,3]. The identification of the order parameter symmetry is an essential issue in current studies of unconventional SC. A common approach to address the symmetry of the order parameter is through investigations of the SC gap, which is expected to have the same symmetry as the order parameter. While progress has been made for high- $T_c$  superconductors (HTSC), the identification of the gap symmetry remains an open question for most HF materials. Unfortunately, the eventual identification of the gap symmetry in a HF compound is not sufficient to identify the pairing mechanism. Additional elements are necessary and in the case of HF materials, it was suggested that spin-fluctuations - either in the itinerant [4,5] or localized limit as magnetic excitons [6,7] - may replace the phonons as mediators of the pairing.

In order to identify the gap symmetry and clarify its relationship to the pairing mechanism, selfconsistent solutions of the SC gap equations with physical momentum dependent pairing potentials and accurate band structures are unavoidable. Such type of calculations have been achieved only recently for HTSC and ruthenates where usually two-dimensionality is assumed and a tight-binding dispersion of one or two electron bands is considered [8–11]. In the case of HF's the situation is much more complex. In addition to the three-dimensionality, we must deal with several anisotropic bands that cross the Fermi level ( $E_F$ ) producing numerous highly anisotropic Fermi surface (FS) sheets. Due to the complicated structure of the bands in HF materials, simple tight-binding fits are impossible to obtain. As a consequence, no realistic selfconsistent calculations of SC

have been achieved so far in HF materials.

Here we report for the first time a direct combination of relativistic band-structure calculations with realistic selfconsistent calculations of SC in a HF material. We focus on  $\text{UPd}_2\text{Al}_3$  which is a fascinating HF superconductor having a moderately large specific heat coefficient  $\gamma = 140 \text{ mJ/mol K}^2$ , and a relatively high critical temperature  $T_c = 2 \text{ K}$  [12]. It orders antiferromagnetically below  $T_N = 14.3 \text{ K}$  with an ordered moment of  $0.85 \mu_B/\text{U-atom}$  [13], which is large compared to the moments of other HF superconductors as, e.g.,  $\text{UPt}_3$ , which has a moment of only  $0.03 \mu_B$ . A further anomalous feature is that the antiferromagnetic (AFM) order coexists with SC below  $2 \text{ K}$ . Coexistence of magnetism and SC was observed for other materials, e.g., containing  $4f$  elements, but in those cases the magnetism is due to the localized  $4f$  electrons far from  $E_F$ , whereas the SC is carried by itinerant electrons at  $E_F$ . Conversely, for  $\text{UPd}_2\text{Al}_3$  most of the recent studies reveal that the SC, magnetic order, as well as HF behavior *all* involve the uranium  $5f$  states [14,15]. Moreover, some striking similarities with cuprate HTSC emerged recently. Neutron scattering experiments [16,17] have reported a distinct resonant mode that develops below  $T_c$  as in HTSC. Tunneling spectroscopy experiments [18] in the SC state reported peculiar dip-hump features in the tunneling spectrum, similar to those observed in HTSC.

We solve selfconsistently the simplified gap equation starting from energy dispersions which we computed within the framework of density-functional theory in the local spin-density approximation (LSDA). In our computational approach we adopt several assumptions. First, we approximate the multiband gap equation [19] by an effective singleband equation. This is justified because the bands at  $E_F$  have mainly  $5f$  character [14], and there is thus no need to discriminate different band characters. The pairing potential is therefore independent

of the band character. In the multiband Hamiltonian [19] the fermion operators for the different band characters become thereby identical, and an effective singleband Hamiltonian, with the energy dispersion  $\epsilon_{\mathbf{k}}$  replaced by  $\sum_n \epsilon_{n\mathbf{k}}$  ( $n$  is the band index), results. We obtain consequently one gap symmetry defined for the whole FS. This corresponds to the experimental studies that identify a global gap symmetry and not one for every FS sheet [15,18,20]. Second, since it is experimentally firmly established that UPd<sub>2</sub>Al<sub>3</sub> is a spin singlet superconductor [21], we explore in our calculations only singlet states. Third, we adopt an *adiabatic* approach in our investigation of the SC order parameter. This means that we neglect the renormalization of the AFM bands by the SC, which is justified because the magnitude of the energy scale of SC is an order of magnitude smaller than that of the AFM order. Fourth, in UPd<sub>2</sub>Al<sub>3</sub> there exist certainly many-particle effects that are responsible for the high effective mass, which can cause a renormalization of the energy bands. Such processes are not taken into account in our LSDA calculations. Previous studies demonstrated a very close correspondence of the measured [22] and calculated [14] de Haas-van Alphen frequencies, and consequently the FS of UPd<sub>2</sub>Al<sub>3</sub> is accurately described by the LSDA energy dispersions. Since the relevant physics for SC happens in the vicinity of the FS, the LSDA bands are the appropriate starting point for the study of the gap symmetry. Moreover, we focus here on a *qualitative* analysis of the gap symmetry avoiding quantitative aspects of SC for which the incorrect values of the effective masses in our LSDA scheme will indeed have some influence.

We computed the energy bands of UPd<sub>2</sub>Al<sub>3</sub> with the relativistic augmented-spherical-wave method [23]. The resulting LSDA band structure of UPd<sub>2</sub>Al<sub>3</sub> along characteristic symmetry lines is shown in Fig. 1 for the paramagnetic and AFM state. The FS resulting from our AFM bands consists of four types of sheets, and is practically identical to that computed previously [14], as is also the ordered AFM moment of 0.81  $\mu_B$ , which agrees with the experimental moment of 0.85  $\mu_B$  [13].

The simplified gap equation in the  $T = 0$  regime is

$$\Delta_{\mathbf{k}} = \frac{1}{2} \sum_{\mathbf{k}'} V(\mathbf{k}, \mathbf{k}') \Delta_{\mathbf{k}'} (X_{\mathbf{k}'} + \Delta_{\mathbf{k}'}^2)^{-1/2}, \quad (1)$$

where  $V(\mathbf{k}, \mathbf{k}')$  is the pairing potential, and  $X_{\mathbf{k}'} = (\sum_n \epsilon_{n\mathbf{k}'})^2$  is the superposition of *all* the relevant bands (dotted lines in Fig. 1). The momentum summation is over the full Brillouin zone (BZ). An unphysical property of Eq. (1) may occur when summed energies are zero, but not the individual energies. To avoid such situation we approximate  $X_{\mathbf{k}} \approx \sum_n \epsilon_{n\mathbf{k}}^2$ . We verified that this approximation did not affect the resulting gap symmetry. We consider two types of pairing kernels that were shown to produce unconventional order parameters. The small- $q$

pairing potential adopts at small wavevectors the following form in momentum space  $V(\mathbf{k}, \mathbf{k}') = \frac{-V}{q_c^2 + (\mathbf{k} - \mathbf{k}')^2} + \mu^*(\mathbf{k} - \mathbf{k}')$ . This kernel is characterized by a smooth momentum cut-off  $q_c$  which selects the small- $q$  processes in the attractive part [8,24–27]. At larger wavevectors the repulsive Coulomb pseudopotential  $\mu^*(\mathbf{k} - \mathbf{k}')$  prevails. This type of attractive interaction may be due to phonons if screening with short range Hubbard-like Coulomb terms is involved [25]. It has been claimed that this type of kernel may account for unconventional SC in HTSC [8,27] and in other materials, including HF's [25]. Agterberg *et al.* [28] have recently suggested for HF superconductors a multipocket FS with an attractive intrapocket and repulsive inter-pocket potential. Such situation results naturally from a potential dominated by small- $q$  attractive pairing as the one considered here, if the FS contains multipockets. We also considered the case of pairing mediated by *spin-fluctuations* using a phenomenological Millis-Monien-Pines pairing potential [29] which has the form  $V(\mathbf{k}, \mathbf{k}') = \frac{V}{q_c^2 + (\mathbf{k} - \mathbf{k}' - \mathbf{Q})^2}$  where  $\mathbf{Q} = (0, 0, \pi/2c)$  in UPd<sub>2</sub>Al<sub>3</sub> ( $c$  is the  $c$ -axis lattice constant). This type of pairing has been suggested for virtually all unconventional SC's, including UPd<sub>2</sub>Al<sub>3</sub> [30,15].

To obtain selfconsistent gap solutions with such momentum dependent kernels we have used a Fast-Fourier-Transform technique. The problem is solved iteratively on a symmetric part of the BZ that we discretize with a  $128 \times 128 \times 128$  momentum grid. For each point of our 3-D grid we have our LSDA energy bands as an input. Within our procedure the momentum space problem is fully resolved numerically without any simplification or bias on the resulting gap symmetry.

In UPd<sub>2</sub>Al<sub>3</sub>, NMR measurements revealed a singlet SC state [21] with a gap of even parity. Because UPd<sub>2</sub>Al<sub>3</sub> and thus our LSDA bands obey the hexagonal  $D_{6h}$  point group symmetry, the only even parity accessible gap states with nodes should transform according to the irreducible representations of  $D_{6h}$  [31] shown schematically in Fig. 2. As a first step in our iteration scheme, the initial gap configuration is chosen randomly and the system is totally free to converge within the iteration cycle towards the most favorable representation. In a second step we bias the system by adopting as initial gap configuration each of these representations and try to force convergence towards the chosen representation. In that way, we check the ground state character of the solution obtained in the first step. The precision of our numerical calculation is such that it allows to distinguish which representation corresponds to the lowest free energy. The lowest-in-energy representation, e.g., has a free energy that is 10% less than the next higher one. The second step in addition allows us to identify any eventual degeneracy between the various accessible gap symmetries.

The central result of our calculations is that the only accessible gap states with nodes in UPd<sub>2</sub>Al<sub>3</sub> *transform*

according to the fully symmetric irreducible representation  $A_{1g}$ . This is true irrespective of the precise momentum structure of the pairing kernel. We show in Fig. 3 some examples of our selfconsistently obtained gap functions in the plane  $L - A - L - L - M - L$  which contains the  $z$ -axis (the  $A - \Gamma - A$  axis) and in the plane obtained by a  $\pi/6$  or  $\pi/2$  rotation around the  $z$ -axis (the plane  $H - A - H - H - K - H$ ). All selfconsistent solutions shown in fig. 3 have two lines of nodes practically perpendicular to the  $A - \Gamma - A$  axis, thus belonging in the  $A_{1g}$  representation. *No other representation possessing nodes was accessible* for all parameters in the pairing kernels that we have investigated. To study the influence of the coexisting AFM order on SC we have made calculations using both paramagnetic and AFM bands. In both paramagnetic and AFM cases, the only solutions with gap nodes are of  $A_{1g}$  type. Note that our results with the spin-fluctuations kernel confirm the model analysis by Huth *et al.* [30].

There is overwhelming experimental evidence that indeed  $\text{UPd}_2\text{Al}_3$  has a gap with the  $A_{1g}$  node structure. Recent tunnel measurements along the  $z$ -axis showed the absence of a node in this direction [18]. However, the presence of nodes is definitely established in  $\text{UPd}_2\text{Al}_3$ , and since  $A_{1g}$  is the only even parity gap with nodes which is nodeless along the  $z$ -direction, it was deduced *a posteriori* that the gap symmetry must be  $A_{1g}$  type [18]. In addition, the observation of a spin-fluctuations peak below  $T_c$  at  $(0, 0, \pi/2c)$  [16,17] would be forbidden by the involved coherence factors unless the gap changes sign along the  $z$ -axis as in the  $A_{1g}$  representation [32]. Finally, measurements of the angular dependence of the critical field indicate two lines of nodes perpendicular to the  $z$ -axis [20] again suggesting the  $A_{1g}$  representation.  $\text{UPd}_2\text{Al}_3$  is perhaps the only HF superconductor for which such a clear picture of the nodal structure of the gap is obtained from the experiments. We consider the agreement of our results with the experiments as strong support of our calculations.

The surprising robustness of the  $A_{1g}$  solution results from the following general rule: If a system must choose a gap symmetry with nodes because of the repulsive effective interaction at large wavevectors (short distances) it chooses *the representation that has the minimum number of nodes as far as possible from the high-density areas*. In fact, the system must *maximize* the condensation free energy and this is obtained when there is a gap in the high-density areas and the node (gapless) areas are kept minimal. Examining the paramagnetic bands of  $\text{UPd}_2\text{Al}_3$  (Fig. 1b) we see that the high-density areas near the FS due to saddle points in the band dispersions are found essentially near the A point and near the H point. The  $A_{1g}$  representation prevails because it is the only one *without a node near the A point*. In the case of the AFM bands (Fig. 1c), the saddle points of the bands near the FS are found essentially in the  $z = 0$  plane (near

the  $\Gamma$  point, along the  $\Gamma - K$ ,  $K - M$  and  $M - \Gamma$  symmetry lines) and near the  $\Gamma$  point along  $\Gamma - A'$  ( $A' = A/2$ ). The high-density areas in the  $z = 0$  plane exclude the  $B_{1g}$ ,  $E_{1g}$  and  $B_{2g}$  representations which have a line node in the  $z = 0$  plane. From the remaining  $A_{1g}$ ,  $E_{2g}$  and  $A_{2g}$  representations,  $A_{1g}$  is the only one without a line of nodes parallel to the  $A - \Gamma - A$  axis which would cross the high-density areas at  $\Gamma$  and near  $\Gamma$  along  $\Gamma - A'$ . Also, due to the AFM symmetry a high density occurs again at A, as A is equivalent to  $\Gamma$ . The node perpendicular to the  $\Gamma - A$  path in the  $A_{1g}$  representation is close to  $A'$  and therefore does not cross the high-density areas near  $\Gamma$  and A. Note that  $A_{2g}$ ,  $B_{1g}$  and  $B_{2g}$  are also handicapped by the fact that they have more nodal areas.

To stress the generality of this argument we reconsidered the case of cuprate HTSC. Saddle points produce high-density areas in the vicinity of  $(0, \pi/a)$  and symmetry related areas ( $a$  is the lattice constant in the basal plane). The  $d_{x^2-y^2}$  gap symmetry corresponds to nodes along the  $(\pi/a, \pi/a)$  direction as far as possible from the high-density  $(0, \pm\pi/a)$  and  $(\pm\pi/a, 0)$  areas. Using both types of pairing kernels as adopted for  $\text{UPd}_2\text{Al}_3$  (now  $\mathbf{Q} = (\pi/a, \pi/a)$ ) we were never able to obtain a  $d_{xy}$  solution for which the nodes cross the high-density  $(0, \pi/a)$  areas *no matter the details of the interaction*.

In conclusion, we have computed the first selfconsistent solutions of SC in the HF material  $\text{UPd}_2\text{Al}_3$ . Our calculations demonstrate that the only even parity accessible gap symmetry with nodes transforms according to the  $A_{1g}$  irreducible representation of the  $D_{6h}$  point group, independent of whether the pairing potential is dominated by small-q attractive processes or by spin-fluctuations. The robustness of the  $A_{1g}$  representation is analyzed to be due to the presence of high-density regions of the relevant bands in the vicinity of the  $\Gamma$  and A points, that preclude node formation at these points. As a general rule we obtain that nodes must be as far as possible from high-density areas in the phase space.

We are grateful to H. Adrian, E.N. Economou, P. Fulde, M. Huth, M. Lang, P. Thalmeier, N. Sato and F. Steglich for illuminating discussions. We thank M. Huth for the figure of the irreducible representations of the  $D_{6h}$  group.

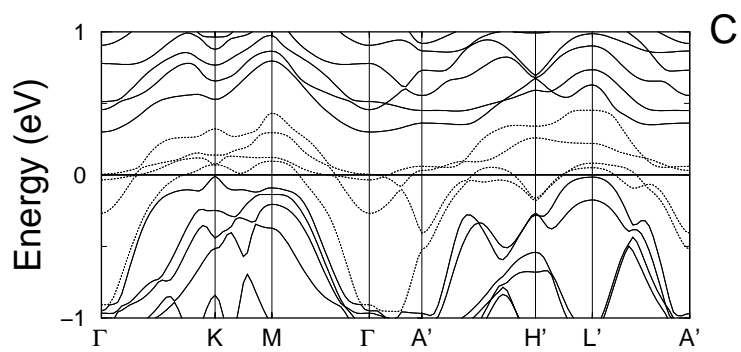
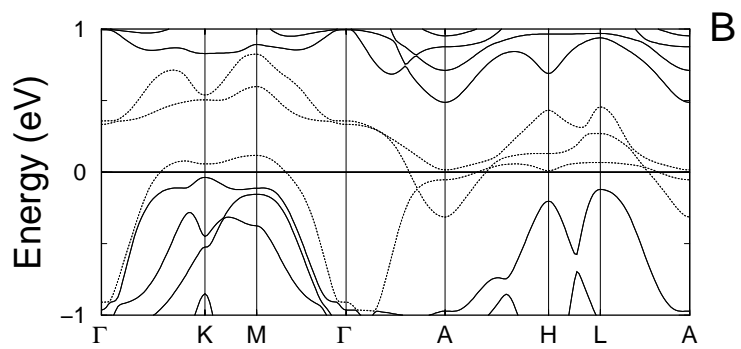
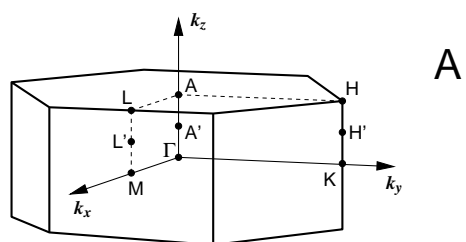
- 
- [1] F. Steglich *et al.*, Phys. Rev. Lett. **43**, 1892 (1979).
  - [2] M. Sigrist and K. Ueda, Rev. Mod. Phys. **63**, 239 (1991).
  - [3] J. F. Annett, Adv. Phys. **39**, 83 (1991).
  - [4] N. D. Mathur *et al.*, Nature **394**, 39 (1998).
  - [5] S. S. Saxena *et al.*, Nature **406**, 587 (2000).
  - [6] P. Coleman, Nature **410**, 320 (2001).
  - [7] N. Sato *et al.*, Nature **410**, 340 (2001).
  - [8] G. Varelogiannis *et al.*, Phys. Rev. B **54**, R6877 (1996).

- [9] W. M. Temmerman *et al.*, Phys. Rev. Lett. **76**, 307 (1996); B. L. Gyorffy *et al.*, Phys. Rev. B **58**, 1025 (1998).
- [10] P. Monthoux and G. Lonzarich, Phys. Rev. B **59**, 14598 (1999).
- [11] G. Litak *et al.*, cond-mat/0105376.
- [12] C. Geibel *et al.*, Z. Phys. B **84**, 161 (1991).
- [13] A. Krimmel *et al.*, Z. Phys. B **86**, 161 (1992).
- [14] K. Knöpfle *et al.*, J. Phys.: Condens. Matter **8**, 901 (1996).
- [15] N. Bernhoeft, Eur. Phys. J. B **13**, 685 (2000).
- [16] N. Metoki *et al.*, Phys. Rev. Lett. **80**, 5417 (1998).
- [17] N. Bernhoeft *et al.*, Phys. Rev. Lett. **81**, 4244 (1998).
- [18] M. Jourdan, M. Huth, and H. Adrian, Nature **398**, 47 (1999).
- [19] H. Suhl, B. T. Matthias, and L. R. Walker, Phys. Rev. Lett. **3**, 552 (1959).
- [20] J. Hessert *et al.*, Physica B **230–232**, 373 (1997).
- [21] M. Kyougaku *et al.*, J. Phys. Soc. Jpn. **62**, 4016 (1993).
- [22] Y. Inada *et al.*, Physica B **189–200**, 119 (1994).
- [23] A. R. Williams, J. Kübler, and C. D. Gelatt, Phys. Rev. B **19**, 6094 (1979).
- [24] A. A. Abrikosov, Phys. Rev. B **53**, R8910 (1996).
- [25] G. Varelogiannis, Phys. Rev. B **57**, 13743 (1998).
- [26] M. Weger and M. Peter, Physica C **317–318**, 252 (1999).
- [27] A. J. Leggett, Phys. Rev. Lett. **83**, 392 (1999).
- [28] D. F. Agterberg, V. Barzykin, and L. P. Gor'kov, Phys. Rev. B **60**, 14868 (1999).
- [29] A. J. Millis, H. Monien, and D. Pines, Phys. Rev. B **42**, 167 (1990).
- [30] M. Huth, M. Jourdan, and H. Adrian, Eur. Phys. J. B **13**, 695 (2000).
- [31] S. K. Yip and A. Garg, Phys. Rev. B **48**, 3304 (1993).
- [32] Such an argument has already been invoked for the  $d_{x^2-y^2}$  symmetry of the gap in the cuprates. See, e.g., H. F. Fong *et al.*, Phys. Rev. Lett. **75**, 316 (1995).

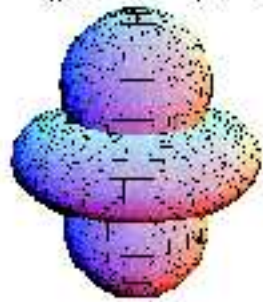
FIG. 1. (a) The hexagonal Brillouin zone with high symmetry points. In the AFM phase the BZ is reduced by a factor two along the  $z$ -axis (denoted by the primed letters). (b) The energy bands along high symmetry directions in the paramagnetic, and (c) the AFM phase of  $\text{UPd}_2\text{Al}_3$ . The relevant bands for superconductivity are shown by the dotted lines.

FIG. 2. The even parity irreducible representations of the  $D_{6h}$  point group. While in principle all are accessible for the gap, only the  $A_{1g}$  results from our selfconsistent gap calculations.

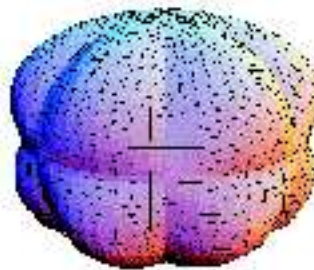
FIG. 3. (color) Some examples of the selfconsistent gap solutions in characteristic planes (with sides indicated) that contain the  $\Gamma$  point (in the center) and the  $z$ -axis ( $A-\Gamma-A$  axis). The thick black lines show the nodes and in the blue areas the gap is negative. All nodes cut the  $A-\Gamma-A$  axis as in the  $A_{1g}$  representation. We show here results obtained with small- $q$  pairing and AFM energy bands, (a and b), spin-fluctuations pairing and AFM bands (c), and small- $q$  pairing and paramagnetic bands (d). In (d) the sign of the gap is inverted to visualize better the variation of the gap.



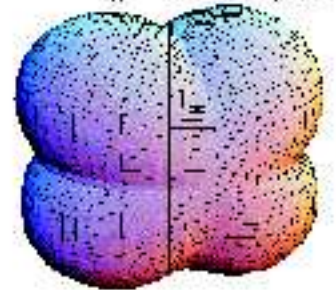
$$A_{1g}: (k_x^2 + k_y^2) - k_z^2$$



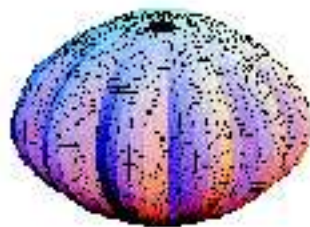
$$B_{1g}: k_z k_x (k_x^2 - 3k_y^2)$$



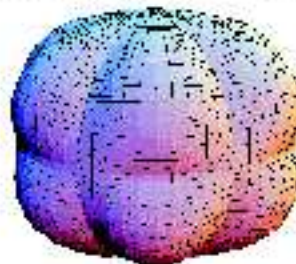
$$E_{1g}: k_x k_z + k_y k_z$$



$$A_{2g}: k_x k_y (k_x^2 - 3k_y^2) (k_y^2 - 3k_x^2)$$



$$B_{2g}: k_z k_y (k_y^2 - 3k_x^2)$$



$$E_{2g}: k_x^2 - k_y^2 + 2 k_x k_y$$

